lisions to be negligible, all relevant lengths must be short compared to the the mean free path of the beam electrons in the plasma. Furthermore, the growth rate γ of the unstable modes must be large compared to the collision frequency of the plasma electrons. However, these conditions do not yet ensure that the resonant effect of thermally excited stable modes on the beam is small compared to the one of the unstable modes considered so far. The importance of this supplementary effect can be estimated starting from Eqs. (1), (3), and (4) with

$$\mathcal{E}_k^{(0)} = mv_{th}^2/\lambda_D^2 \quad \text{for all } x \text{ and } t.$$

Thus one obtains, using the approximation (6),

$$f(x, v, t) = \frac{8\omega_p}{m}\frac{mv_{th}^2}{\lambda_D^2}\, x\, \frac{1}{v}\frac{\partial}{\partial v}\left(\frac{\gamma^{(0)}_{(\omega_p/v)}}{v^3}\right) + f(x = 0, v, t - x/v)$$

for the entire interval $0 < x < vt$ where beam electrons of velocity v are present. Along the lines of the preceding section, it can be shown that the variation of the moments $M(\alpha)$ and of the mean values $\langle v^\alpha \rangle$, due to the resonant thermal noise, are again given by Eqs. (13) and (15), however, replacing φ by

$$\bar{\varphi} = 8\lambda/\delta\beta^3 N\lambda_D^3. \tag{21}$$

The validity of this result is limited to such values of λ such that $\bar{\varphi} \ll 1$ holds, i.e.,

$$\lambda \ll \tilde{\Lambda} \equiv \tfrac{1}{8}\delta\beta^3 N\lambda_D^3. \tag{22}$$

$\tilde{\Lambda}$ represents the penetration depth of the front of a beam which is affected only by the thermal noise.

If $t < t_0$, the effect of the resonant thermal noise is neglibible for $\bar{\varphi} \ll \varphi$. When $\bar{\varphi} \gg \varphi$ this effect dominates that of the unstable modes. The results obtained in Sec. 3 are, hence, limited to distances such that

$$\exp\left(\frac{2\beta^3}{3\delta^2}\frac{n_0}{N}\lambda\right) - 1 > \frac{2\beta^7}{3\delta^4}\frac{n_0}{N}\lambda \tag{23a}$$

in the stationary range $0 < \lambda < 3\tau/\beta$ and, within the limits of condition (19), to values of σ such that

$$\sigma > \frac{N\delta^2(\beta^2 - 3)}{2n_0\beta^4}\ln\frac{2\beta^7(n_0/N)\lambda}{[3\delta^2 + 2\beta^3(n_0/N)\lambda]\delta^2} \tag{23b}$$

in the nonstationary range. This last relation essentially corrects and makes more stringent the lower limit for σ as given by (19). For $\Lambda < \lambda < \tilde{\Lambda}$ there is, however, still a finite interval of σ where the results of Sec. 3 apply. Equation (23a), on the other hand, limits the distances $\lambda < \Lambda$ from below where the model holds for all τ larger than a minimum value defined by $\bar{\varphi} = \varphi$. This limit λ_0 tends to zero if the transverse size of the unstable domain is so large that $\Delta k \to \lambda_D^{-1}$, or equivalently $\delta \to \beta^2$. Then, all resonant modes, appreciably excited in thermal equilibrium are also unstable and hence these describe the relevant excitation throughout quite well.

In Fig. 5 a schematic plot of the different ranges appearing in the preceding discussion is shown. A numerical example has been given elsewhere.[5]

In a finite system the previous results may be modified by the effect of the second plasma boundary. Whereas in general the beam will be destroyed there so that the boundary condition (4) also remains valid in this case, there may be complete or partial reflection of the modes strongly excited by the instability. These then travel back to the first boundary and might alter the boundary condition (5) for times larger than about $(1/u + u/3v_{th}^2)D$ where D is the thickness of the system. This does not happen, however, if the Landau damping of these waves is strong enough to reduce their excitation to the thermal level when they again reach the first boundary. This is generally the case in situations slightly above the onset of the instability; it may be also true, however, in other situations, e.g., if there is a strong absorption of the unstable modes at the second plasma boundary, or if D is large compared to the penetration depth $L = \Lambda\lambda_D$ of the beam so that the ratio of the space intervals effective for amplification and damping, respectively, which is of order L/D, is small. In these cases the above results can also be applied directly to a finite system.

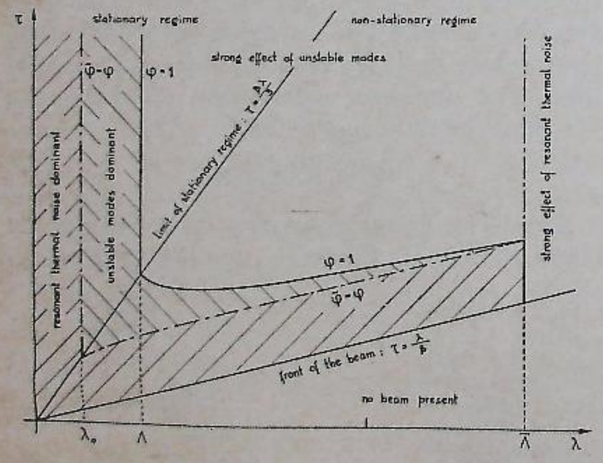

FIG. 5. Schematic plot of the different domains discussed in Secs. 3 and 4 for $0 < t < t_0$; the range of validity of the given approach is hatched.

[5] M. Carnevale, B. Crosignani, and F. Engelmann: Laboratorio Gas Ionizzati Report No. LGI 66/6 (1966).

Velocity Space Instabilities in a Toroidal Geometry

H. L. BERK* AND A. A. GALEEV†
International Centre for Theoretical Physics, International Atomic Energy Agency, Trieste, Italy
(Received 8 August 1966; final manuscript received 24 October 1966)

A self-consistent equilibrium is derived for a simple toroidal model from knowledge of the particle orbits. This equilibrium is investigated for velocity space instabilities analogous to the loss cone of mirror machines. An ion instability generated by particles in "trapped" or nearly "trapped" orbits is found when the rotational transform is relatively weak, but is stabilized with larger rotational transform. Instability is also found at the plasma edge due to a loss of particles in a preferred region of velocity space. A qualitative discussion of the quasi-linear development of these instabilities is presented.

I. INTRODUCTION

RECENTLY it has been realized that a plasma equilibrium can be inherently unstable to velocity space instabilities because of the nature of the confinement. For example, Post and Rosenbluth[1,2] have shown that, because open-ended systems have velocity loss cones, serious electrostatic instability arises at sufficiently high density. Galeev[3] has shown that this instability causes particles to diffuse into the loss cone of the machine. Thus, instability is present because confined particles are relaxing to fill unoccupied regions of phase space.

Similarly, one can ask if velocity space instabilities are likely to arise in a toroidal equilibrium. Certainly a toroidal equilibrium seems more stable in this respect than a mirror geometry, since toroidal fields with rotational transform and nested magnetic surfaces form an ideal container in that all particle trajectories are bounded.[4,5] However, even for a toroidal system there can be regions of phase space where the equilibrium distribution has steep velocity space gradients which may give rise to instability.

The most obvious region is near the walls of the container. Since particles with different velocities displace differently from a given magnetic surface, velocity space holes will develop near the edge for those particles whose trajectories have maximum displacement. Thus, as noted by Bishop and Smith,[6] an escape region analogous to the loss cone of a mirror machine is present.

Another important region in phase space is the boundary between orbits of different topologies, i.e., between particles whose sense of velocity along the torus is fixed and those that have mirror orbits (trapped particles). Because of the topological difference of the trajectories, anomalously large velocity space gradients may be present in the distribution function which can supply a mechanism for instability.

In this paper we investigate some of these velocity space micro-instabilities inherent in a toroidal configuration. To this end a model toroidal equilibrium is developed from the study of particle trajectories and investigated in detail. The recent numerical work of Bishop and Smith[6] studied an equilibrium of a model similar to ours. In their work the particle displacement is a sizable fraction of the minor radius so that a large escape region exists and a large velocity space hole is formed. Therefore, many particles are lost directly to the wall, so that a large electric field throughout the plasma exists which results in a complicated equilibrium. In our case we assume that the particle displacement is relatively small, as would be the case of a future device needed for fusion. Therefore the effect of the boundary is not as pronounced and the equilibrium is not unduly complicated.

We find that, to lowest order, the macroscopic nature of our equlibrium agrees with fluid results. However, we find that although higher-order effects do not significantly modify the fluid equilibrium, they supply mechanisms for micro-instabilities. It is shown that because a velocity space hole develops due to particle loss to the wall, the plasma is unstable near the wall. Similarly, if the rotational transform

* Permanent address: University of California, San Diego, La Jolla, California.
† Permanent address: Institute for Nuclear Physics, Novosibirsk, U.S.S.R.
[1] R. F. Post and M. N. Rosenbluth, Phys. Fluids 8, 547 (1965).
[2] R. F. Post and M. N. Rosenbluth, Phys. Fluids 9, 730 (1966).
[3] A. A. Galeev, Zh. Eksperim. i Teor. Fiz. 49, 672 (1965) [English transl.: Soviet Phys.—JETP 22, 466 (1966)].
[4] S. A. Morozov and L. S. Solovyev, Zh. Techn. Fiz. 30, 271 (1960). [English transl.: Soviet Phys.—Tech. Phys. 5, 250 (1960)].
[5] S. A. Morozov and L. S. Solovyev, Dokl. Akad. Nauk SSSR 128, 506 (1959) [English transl.: Soviet Phys.—Doklady 4, 1031 (1960)].
[6] A. S. Bishop and C. G. Smith, Phys. Fluids 9, 1380 (1966).

is too small, the trapped particle region of velocity space gives rise to instability. We conclude the paper with a qualitative discussion of the quasi-linear implications of these instabilities.

II. TOROIDAL MODEL AND PARTICLE TRAJECTORIES

For our toroidal geometry we consider the system illustrated in Fig. 1. The system is assumed symmetric about the toroidal axis (A, B), the (r, ϕ) plane contains the toroidal axis and the z direction is taken perpendicular to the (r, ϕ) plane. R is the mean major radius, a is the minor radius, and $a/R \ll 1$. The main magnetic field is taken as that due to a current along the toroidal axis, and hence is given by $\mathbf{B} = B_0[1 - (r/R)\cos\phi]\hat{\mathbf{Z}}$. An additional field, $\Delta\mathbf{B} = -\iota(r/R)B_0\hat{\phi}$, causes a rotational transform ι, about the center of the minor circle. The rotational transform is taken as a function of r only, as if a hard core or internal currents were present. We neglect the effect of $\Delta\mathbf{B}$ on the magnitude of B since it is a quantity of $O[(r/R)^2]$. We see that the magnetic surfaces are given by $r = \text{const}$. For pure cylindrical geometry, the guiding center is fixed at a given r, but in toroidal geometry we show that the particle trajectories can deviate from a fixed magnetic surface.

Because of the symmetry in the z direction, it is sufficient to consider the projection of the particle motion upon an (r, ϕ) plane. We assume that the electric potential, $\Phi(r)$, is a function of r only, and the electric field drift is much less than the particle's speed. Hence the equations of motion of the guiding centers of a specie of charge e and mass m take the form,

$$\frac{dr}{dt} = -\frac{(\frac{1}{2}v_\perp^2 + v_\parallel^2)\sin\phi}{\omega_c R}, \tag{1}$$

$$r\frac{d\phi}{dt} = -\frac{(\frac{1}{2}v_\perp^2 + v_\parallel^2)}{\omega_c R}\cos\phi + \frac{e}{m\omega_c}\frac{\partial\Phi}{\partial r} - \frac{\iota v_\parallel r}{R}, \tag{2}$$

where $v_\perp$ and $v_\parallel$ are the velocity components perpendicular and parallel to the magnetic field, and $\omega_c = eB_0/mc$ is the gyrofrequency. The right-hand side of Eq. (1) is the r component of the grad B and curvature drifts while the right-hand side of Eq. (2) are, respectively, the ϕ components of the grad B and curvature drifts, the electric field drift and rotation due to the rotational transform. In these equations terms of order $(r/R)^2$ have been neglected. Combining Eqs. (1) and (2), we obtain

$$\frac{(\frac{1}{2}v_\perp^2 + v_\parallel^2)}{\omega_c R}\frac{d}{dr}(r\cos\phi) = -\frac{\iota v_\parallel r}{R} + \frac{e}{m\omega_c}\frac{\partial\Phi}{\partial r}. \tag{3}$$

Now since $E = \frac{1}{2}(v_\perp^2 + v_\parallel^2) + [e\Phi(r)/m]$ and $\mu = v_\perp^2/2B(r)$ are constants of motion, we have

$$\frac{e}{m}\frac{\partial\Phi}{\partial r} = -v_\parallel\frac{dv_\parallel}{dr} + \frac{\mu B}{R}\frac{d}{dr}(r\cos\phi) + O\left(\frac{r^2}{R^2}\right), \tag{4}$$

where $v_\parallel(r) = \pm\{2[E - \mu B(r) - (e/m)\Phi(r)]\}^{\frac{1}{2}}$. From this relation, we find that Eq. (3) can be written as

$$\frac{v_\parallel}{\omega_c R}\frac{d}{dr}(r\cos\phi) = -\frac{\iota r}{R} - \frac{1}{\omega_c}\frac{dv_\parallel}{dr}. \tag{5}$$

Now if $dv_\parallel/dr \ll v_\parallel/r$ (which is the case if $(e/m\omega_c)(d\Phi/dr) \ll v_\parallel$ or $v_\perp$), the r dependence of $v_\parallel$ can be neglected on the left-hand side of the equation. We then readily integrate Eq. (5) and obtain an additional constant of motion,

$$J = \frac{\omega_c}{R}\int_0^r \iota r\,dr + v_\parallel\left(1 + \frac{r}{R}\cos\phi\right). \tag{6}$$

This quantity is analogous to the usual longitudinal invariant, but now we see that for our model it is an exact constant of motion (at least to the extent that μ is constant).

If we assume that the particle displacement is small, which we shall see is satisfied if $r_L/\iota r \ll (r/R)^{\frac{1}{2}}$, where r_L is the Larmor radius, the particle trajectories are easily traced. Starting with the point (r_0, ϕ_0) as reference, and expanding Eq. (6) to second order in $(r - r_0)$, we obtain the equation

$$\tfrac{1}{2}(\omega_c\theta^2 - v_\parallel\theta' + v_E')(r - r_0)^2 - \Delta v\theta(r - r_0) - v_s r(\cos\phi - \cos\phi_0) = 0, \tag{7}$$

where

$$\Delta v = v_\parallel - v_E/\theta,$$

$$v_\parallel = \pm\{2[E - \mu B - (e/m)\Phi(r_0)]\}^{\frac{1}{2}},$$

$$\theta = \frac{\iota r}{R}\bigg|_{r=r_0}, \qquad v_E = \frac{e}{m}\frac{\partial\Phi}{\partial r}\frac{1}{\omega_c},$$

$$v_s = \frac{\mu B_0 + v_\parallel^2}{\omega_c R}.$$

If Δv is not too small, we see that the displacement is given by

$$(r - r_0) = -[(\mu B_0 + v_\parallel^2)/\Delta v\omega_c R](\cos\phi - \cos\phi_0)r_0.$$

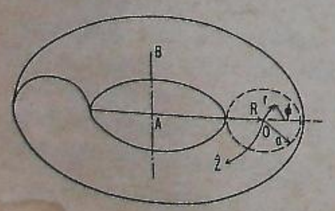

FIG. 1. Toroidal coordinates.

A positively charged particle circulates around the cross section of the torus in a clockwise direction for $\Delta v > 0$ and counterclockwise for $\Delta v < 0$ [see Fig. 2(a) where the reference points $(r_0, \phi_0) = (r_0, 0)$].

The general solution to Eq. (7),

$$(r - r_0) = \frac{\Delta v \pm \left[(\Delta v)^2 + 2r\left(\omega_c - \frac{\theta'}{\theta^2}v_\parallel + \frac{v_E'}{\theta^2}\right)v_s(\cos\phi - \cos\phi_0)\right]^{\frac{1}{2}}}{(\omega_c\theta - v_\parallel\theta'/\theta + v_E'/\theta)}$$

shows that the particle can be trapped if

$$(\Delta v)^2 < 4v_s r(\omega_c - v_\parallel\theta'/\theta^2 + v_E'/\theta^2) \doteq 4v_s r[\omega_c + (v_E/\theta)'/\theta].$$

[For simplicity we assume $\omega_c\theta \gg (v_E/\theta)'$. This inequality is certainly true for a sufficiently large rotational transform or small electric fields.] The trapped motion is about $\phi = 0$ as shown in Fig. 2(b). The maximum displacement occurs for a barely trapped particle which at $\phi = 0$ is

$$r - r_0 = 4(\mu B_0 r/R)^{\frac{1}{2}}/\omega_c\theta.$$

For a barely untrapped particle, the maximum displacement occurs at $\phi = \pi$, where

$$(r - r_0) = 2(\mu B_0 r/R)^{\frac{1}{2}}/\omega_c\theta.$$

The physical picture for the motion is that the drifts cause the particle to move downward. As the particle moves around the magnetic surface, it moves away from the surface when it is below the midplane and towards the magnetic surface when it is above. The maximum displacement occurs for particles that take the longest to cross the midplanes. Similar results have been obtained by Morosov and Solovjev[4,5] for more general toroidal geometries. However, our results are qualitatively correct for particle orbits in a general toroidal geometry.

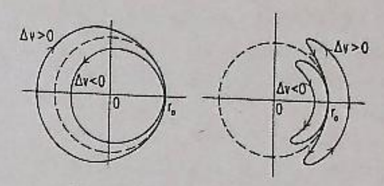

FIG. 2. Particle trajectories.

III. EQUILIBRIUM

We now investigate the equilibrium both far from and near the walls of the torus. We show that the macroscopic nature of the equilibrium is well described by a simple fluid model. However, since we are interested in possible velocity space instabilities, we also look in detail into the equilibrium resulting from a kinetic description.

A. Fluid Model

In the fluid model the fields due to toroidal curvature are mocked by a gravity field $\mathbf{g}_j = \hat{\mathbf{x}}2v_{thj}^2/R$ for the jth specie, where v_{thj} is the thermal velocity and $\hat{\mathbf{x}} = \hat{\phi}$ when $\phi = 0$. The pressure P_j is given by $P_j = nm_j v_{thj}^2$, and the magnetic field is given by $\mathbf{B} = B_0\hat{\mathbf{z}} + B_\phi\hat{\phi}$, where $B_\phi = (\iota r)/RB_0$. The equilibrium equations for a given specie are (the subscripts are now suppressed)

$$-v_{th}^2\nabla n + n\mathbf{g} - ne[\partial\Phi(r)/\partial r]\hat{\mathbf{r}} + (n\omega_c/B_0)(\mathbf{v}\times\mathbf{B}) = 0, \tag{8}$$

$$\nabla\cdot(n\mathbf{v}) = 0. \tag{9}$$

Since we look for an equilibrium independent of z, the z component of Eq. (8) yields $v_r = 0$. Hence from Eq. (9) $\partial/\partial\phi(nv_\phi) = 0$, and hence $nv_\phi = j_\phi(r)$. The ϕ component of Eq. (8) yields

$$n(r, \phi) = n_0(r)\exp\{2(r/R)\cos\phi - [e\Phi(r)/mv_{th}^2]\}, \tag{10}$$

where $e^{-e\Phi(r)/mv_{th}^2}$ is an integration constant explicitly displayed for convenience. From the r component of Eq. (8) we have

$$\omega_c j_\phi(r) = \exp\left(\frac{2r}{R}\cos\phi - \frac{e}{m}\frac{\Phi}{v_{th}^2}\right)v_{th}^2\frac{\partial n_0}{\partial r} + \omega_c n v_z\frac{B_\phi}{B_z}. \tag{11}$$

Since the left-hand side is independent of ϕ, $nv_z \equiv j_z$ must cancel the ϕ-dependence of the first term. Hence, expanding r/R, we find

$$j_\phi(r) = \frac{v_{th}^2}{\omega_c}\frac{\partial n_0}{\partial r}\exp(-e\Phi/mv_{th}^2) \quad \text{(diamagnetic current)}, \tag{12}$$

$$j_z = \frac{2\cos\phi}{\omega_c}v_{th}^2\frac{\partial n_0}{\partial r}\exp(-e\Phi/mv_{th}^2) \quad \text{(rotational transform current)}. \tag{13}$$

B. Kinetic Equilibrium

For a kinetic equilibrium any function of the constants of motion will produce a valid equilibrium. The constants of motion are E, μ, and J. In addition $\sigma = \pm 1$, the sign of $v_\parallel$ a is constant of motion for untrapped particles. We would like to choose an equilibrium that recovers as much as possible the fluid results and is in some sense close to a cy-

lindrically symmetric equilibrium. First, we discuss the problem with $\Phi(r) = 0$.

A convenient distribution function for untrapped particles is

$$f = F(E, \mu) \int_0^{2\pi} \frac{d\phi_0}{2\pi} \int_0^a dr_0\, n(r_0)\ \delta(J - J_\sigma) \left|\frac{\partial J_\sigma}{\partial r_0}\right|. \tag{14}$$

Here,

$$J_\sigma = \frac{\omega_c}{R} \int_0^{r_0} v_\perp\, dr + \sigma\{2[E - \mu B(r_0, \phi_0)]\}^{\frac{1}{2}}\left(1 + \frac{r_0}{R}\cos\phi_0\right),$$

$$B(r, \phi) = B_0\left(1 - \frac{r}{R}\cos\phi\right), \quad \text{and} \quad F(E, \mu),$$

which in general can be taken as an arbitrary function of E and μ, is chosen here as Maxwellian

$$F = \frac{1}{(2\pi v_{\text{th}}^2)^{\frac{3}{2}}} \exp(-E/v_{\text{th}}^2).$$

The weighting factor, $n(r_0)$, is the guiding center density for a purely cylindrical system and is decreasing with increasing r_0. The distribution function has been chosen so that at a given point r, ϕ, for constant E, μ, J, the distribution is influenced by all other points (r_0, ϕ_0) accessible to the particle trajectory. The factor a is the outer radius of the torus. In this section only those trajectories that do not intersect the wall are considered. In Sec. IV we also consider the equilibrium attained when particles intersect the wall and are then lost to the system.

For trapped particles, Eq. (14) is not valid since σ is no longer a constant of motion, and a distribution function independent of σ must be chosen.[7] A distribution function that appears to be the natural choice is $[-\mu B_0(r/R) < E - \mu B_0 < \mu B_0 r/R]$

$$f = \frac{F}{2} \int_{-\frac{1}{2}\phi_m}^{\frac{1}{2}\phi_m} \frac{d\phi_0}{\phi_m} \int_0^a dr_0\, n(r_0) \sum_\sigma \delta(J - J_\sigma) \left|\frac{\partial J_\sigma}{\partial r_0}\right|, \tag{15}$$

where

$$\phi_m = 2\cos^{-1}[(\mu B_0 - E)R/\mu B_0 r_0]$$

is the angle enclosed by a trapped particle.

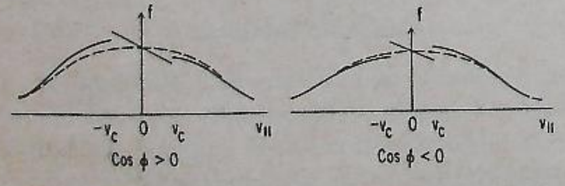

FIG. 3. Distribution function without electric field.

[7] J. Hastie, J. B. Taylor, and F. Haas, Ann. Physik (to be published).

The (r_0, ϕ_0) integrals can be computed by expanding $n(r_0)$ about $n(r)$, if

$$(r - r_0)_{\max} \frac{d}{dr_0} \ln [n(r_0)] \ll 1.$$

Then $n(r_0) = n(r) - n'(r)(r - r_0)$ and the condition $J = J_\sigma$ determines $r - r_0$,

$$r - r_0 = \frac{R}{\iota\omega_c r}\left\{-v_\parallel\left(1 + \frac{r}{R}\cos\phi\right) + \sigma\left(1 + \frac{r}{R}\cos\phi_0\right)\left[2\left(E - \mu B_0 + \frac{\mu B r}{R}\cos\phi_0\right)\right]^{\frac{1}{2}}\right\}. \tag{16}$$

Far from the trapped region we have

$$\overline{(r - r_0)} \equiv \int \frac{d\phi_0}{2\pi} \int dr_0 (r - r_0)\ \delta(J - J_\sigma)\ |J'_\sigma| \tag{17a}$$

$$= -\frac{(\frac{1}{2}v_\perp^2 + v_\parallel^2)\cos\phi}{\iota\omega_c v_\parallel},$$

while for nearly trapped particles we have

$$\overline{(r - r_0)} = \frac{R}{\iota\omega_c r}\left[-v_\parallel + \sigma\left(\frac{2\mu B_0 r}{R}\right)^{\frac{1}{2}} \cdot \int_0^{2\pi} \frac{d\phi_0}{2\pi}\left(\frac{(E - \mu B_0)R}{\mu B_0 r} + \cos\phi_0\right)^{\frac{1}{2}}\right], \tag{17b}$$

where the integral can be expressed in terms of the Legendre function $P_{\frac{1}{2}}$. For trapped particles the term in σ is summed and we obtain

$$\overline{r - r_0} = -\frac{R}{\iota\omega_c r} v_\parallel. \tag{17c}$$

There is a discontinuity in $\overline{(r - r_0)}$ at the transition point $E - \mu B_0 = \mu B_0 r/R$. The limit of $\overline{r - r_0}$ for untrapped particles is

$$\overline{r - r_0} = -\frac{2\sigma}{\omega_c}\left(\frac{\mu BR}{r}\right)^{\frac{1}{2}}\left(|\cos\tfrac{1}{2}\phi| - \frac{2}{\pi}\right), \tag{18a}$$

while for trapped particles

$$\overline{r - r_0} = -(\text{sg}\, v_\parallel)(2/\omega_c)(\mu BR/r)^{\frac{1}{2}}\ |\cos\tfrac{1}{2}\phi|. \tag{18b}$$

The shape of the distribution function $f = [n(r) - \overline{(r - r_0)}n'(r)]F$ for constant $v_\perp$ is shown by the solid lines of Fig. 3. The dotted line is $f = n(r)F$ and $v_c = 2(\mu B_0 r/R)^{\frac{1}{2}}$. Although this analysis is for a special example, the discontinuity at v_c seems quite natural since the topology of the orbits change at this point.[5]

Since r previously referred to guiding center position, we let $\mathbf{r} \to \mathbf{r} - \mathbf{b}\times\mathbf{v}/\omega_c(\mathbf{b} = \mathbf{B}/|\mathbf{B}|)$ so that now r is the actual particle coordinate, and hence $n(r) \to n(r) + n'(v_\perp/\omega_c)\sin(\psi - \phi)$ (ψ is the velocity polar coordinate). The correction to $n'(r)$ is a higher-order effect and is neglected. Our distribution function is then

$$f = \frac{\exp(-E/v_{\text{th}}^2)}{(2\pi v_{\text{th}}^2)^{\frac{3}{2}}} \cdot\left[n(r) - n'\left(\overline{(r - r_0)} - \frac{v_\perp}{\omega_c}\sin(\psi - \phi)\right)\right]. \tag{19}$$

If we now construct the macroscopic moments, we find from symmetry that the particle density remains $n(r)$ while the diamagnetic current, j_ϕ, is given by Eq. (12). If for $r - r_0$, Eq. (17a) is used, we obtain Eq. (13) for j_z. It can be shown that the correction to j_z due to particles near the trapped region is small, $O[(r/R)^{\frac{1}{2}}]$.

The equilibrium with an electric field is constructed in much the same way. For untrapped particles we choose the same distribution function as Eq. (14). If we expand $n(r_0) = n(r) - (r - r_0)n'(r_0)$, we see that the distribution function is given by

$$f = \frac{\exp(-E/v_{\text{th}}^2)}{(2\pi v_{\text{th}}^2)^{\frac{3}{2}}}\left[n(r) - \frac{n'(r)}{\omega_c\theta}\left(\Delta v - \int_0^{2\pi}\frac{d\phi}{2\pi} \cdot [(\Delta v)^2 + 2\omega_c\theta v_\sigma r(\cos\phi - \cos\phi_0)]^{\frac{1}{2}}\right)\right]. \tag{20}$$

Far from resonance this form goes to

$$f = \frac{\exp(-E/v_{\text{th}}^2)}{(2\pi v_{\text{th}}^2)^{\frac{3}{2}}}\left(n(r) + \frac{n'(r)}{\theta\,\Delta v} r v_\sigma \cos\phi\right). \tag{21}$$

We see from Eq. (20) that particles are trapped if the argument of the square root can be less than zero for some ϕ. In this case Eq. (14) cannot be chosen as the distribution function. Instead we choose a distribution function of the form

$$f = \frac{\exp(-E/v_{\text{th}}^2)}{(2\pi v_{\text{th}}^2)^{\frac{3}{2}}}\left(\int_{-\frac{1}{2}\phi_m}^{\frac{1}{2}\phi_m}\frac{d\phi}{2\phi_m} \cdot \int dr_0\ \delta(J - J_\sigma)\ |J'_\sigma|\, n(r_0)\right), \tag{22}$$

where ϕ_m is the angle enclosed by the trapped particles. Performing the integration, we obtain

$$f = \frac{\exp(-E/v_{\text{th}}^2)}{(2\pi v_{\text{th}}^2)^{\frac{3}{2}}}\left(n(r) - \frac{n'\,\Delta v}{\theta\omega_c}\right). \tag{23}$$

The shape of the distribution function is shown in Fig. 4. Note that the resonance velocity $v_\parallel = V_E/\theta$ is the same for electrons and ions.

IV. STABILITY ANALYSIS

Let us now analyze the equilibrium distribution functions we have derived for micro-instabilities.

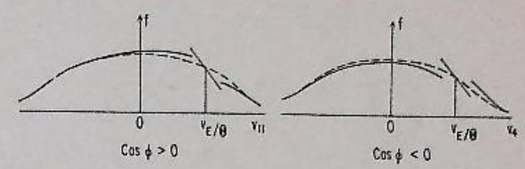

FIG. 4. Distribution function with electric field.

First we look at the distribution function in the body of the plasma and then near the wall.

A. Far from Wall

The simplest type of mode to investigate is electrostatic waves propagating along the magnetic field. For such a mode only the distribution function averaged over $v_\perp$ is needed. When the distribution shown in Fig. 3(a) is averaged, a distribution shaped as in Fig. 5 is obtained. The typical velocity width, δv_i, of the structure is $\delta v_i = v_{\text{th}i}(2r/R)^{\frac{1}{2}}$, while the typical depth, α_i, is

$$\alpha_i = \frac{r_{Li}}{\theta}\frac{r}{L}\left(\frac{2}{rR}\right)^{\frac{1}{2}},$$

where $L = [(d/dr)\ln n(r)]^{-1}$.

We see that the structure is more pronounced for ions than electrons, and hence we consider the averaged electron distribution function as a smooth Maxwellian, while for the ions we choose an averaged distribution function of the form

$$\bar{f}_i = \frac{1}{(2\pi v_{\text{th}i})^{\frac{3}{2}}}\left(\exp(-v_\parallel^2/2v_{\text{th}i}^2) - \frac{\alpha_i v_\parallel}{\delta v_i}\exp[-v_\parallel^2/2(\delta v_i)^2]\right). \tag{24}$$

The dispersion relation is then

$$1 - \sum_i \frac{\omega_{pi}^2}{k^2}\int \frac{dv\ \partial f_i/\partial v}{v - \omega/k} = 0, \tag{25}$$

where ω_{pi}^2 is the plasma frequency for the jth specie. If we look for phase velocities much less than the ion thermal velocity but much greater than δv_i, we find

$$k^2 + \kappa_i^2 + \kappa_e^2 = -\frac{\alpha_i\omega_{pi}^2}{v_{\text{th}i}\ \delta v_i(2\pi)^{\frac{1}{2}}}\int_{-\infty}^{\infty}\frac{dv\, v\exp[-v^2/2(\delta v_i)^2]}{(v - \omega/k)^2} = -2\frac{\alpha_i\omega_{pi}^2}{\omega^3}k^3\frac{(\delta v_i)^2}{v_{\text{th}i}}, \tag{26}$$

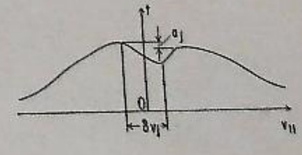

FIG. 5. Averaged distributio

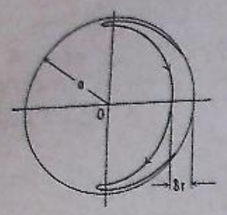

FIG. 6. Trajectory near wall.

where $\kappa_i = \omega_{pi}/v_{thi}$ and $\kappa_e = \omega_{pe}/v_{the}$ are the Debye wave numbers for ions and electrons.

Solving for ω, we obtain as the unstable mode

$$\omega = \frac{(1 + i\sqrt{3})k}{2}\left(\frac{2\alpha_i(\omega_{pi}\ \delta v_i)^2}{(k^2 + \kappa_i^2 + \kappa_e^2)v_{thi}}\right)^{\frac{1}{3}}. \tag{27}$$

If we take $k \sim \kappa_i \sim \kappa_e$, we find the growth rate

$$\gamma \sim \omega_p(\alpha_i\ \delta v_i^2/v_{thi}^2)^{\frac{1}{3}}.$$

For consistency we need $\omega/k \gg \delta v_i$ or

$$\frac{\omega}{\delta v_i k} \simeq \left(\frac{v_{thi}}{\delta v_i}\alpha_i\right)^{\frac{1}{3}} \doteq \left(\frac{r_{Li}R}{\iota r L}\right)^{\frac{1}{3}} > 1. \tag{28}$$

Thus the plasma is unstable if $r_{Li}R/\iota r L > 1$. One can also derive this condition from the Penrose criterion.[8]

Present devices like the C stellerator are susceptible to this instability, but future devices with larger rotational transform can easily avoid this instability.

If the density gradient is very steep, this instability can even be triggered by the electron distribution. The stability criterion, Eq. (28), remains valid but now with the electron Larmor radius present.

Another instability can develop if $T_e \gg T_i$ so that ion-acoustic waves can propagate. If we define V_e as

$$\left.\frac{\partial f_e}{\partial v_\parallel}\right|_{v_\parallel=0} = -\frac{V_e}{v_{the}^2} f_e(v_\parallel = 0),$$

then we see from Eqs. (21)–(23) that

$$V_e \doteq \frac{1}{n}\frac{dn}{dr}\frac{v_{the}^2}{2\omega_{ce}\theta}.$$

It is known that the ion acoustic mode is unstable[9-10]

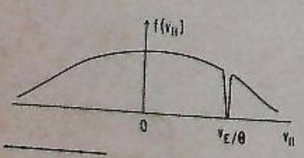

FIG. 7. Distribution near wall.

[8] O. Penrose, Phys. Fluids 3, 258 (1960).
[9] I. B. Bernstein, E. A. Frieman, R. M. Kulsrud, and M. N. Rosenbluth, Phys. Fluids 3, 136 (1960).
[10] E. A. Jackson, Phys. Fluids 3, 786 (1960).

if

$$V_e > (T_e/m_i)^{\frac{1}{2}}$$

(where T_i is the temperature), or

$$(r_e/L\theta)(m_i/m_e)^{\frac{1}{2}} > 1. \tag{29}$$

This condition is almost the same as the previously derived condition.

B. Stability near Walls

The nature of the plasma near the wall requires special analysis. The calculations of the particle trajectories show that the toroidal geometry is an absolute trap in that all particles remain in a restricted region of velocity and coordinate space. However, particles near the wall can intersect the wall and be lost to the system. Because of the particle loss a charge imbalance develops, and thus there will be electric fields near the wall. The magnitude of this electric field is estimated later. We have seen that those particles whose longitudinal velocity are $v_\parallel = c\Phi'(a)/\theta B \equiv v_E/\theta$, where $\Phi(a)$ is the potential at the wall, have a very small azimuthal drift velocity v_ϕ. Thus these particles have the largest deviation from a magnetic surface. We know that the typical displacement of the resonant particle is

$$\delta r_i = (r_{Li}/\theta)(2r/R)^{\frac{1}{2}}$$

and that the resonance is confined to a width $\delta v_i = v_{thi}(2r/R)^{\frac{1}{2}}$. Thus, as shown in Figs. 6 and 7, in the region in coordinate space within δr_i from the wall the resonant particles are lost to the system and a hole in velocity space develops. Particles outside the resonant region but within δr_i are assumed to remain in the torus since their displacement from a magnetic surface is small.

Although a hole in velocity space is an acceptable equilibrium, we expect that it is filled rapidly either by Coulomb collisions or instabilities. In fact, the role of collisions cannot be entirely ignored since we are now dealing with a distribution function with large gradients in velocity space. This can be seen directly from the linearized structure of Landau's collision operator,[11]

$$St\{f_i\} \doteq \frac{v_{thi}^2}{\tau_{ci}}\frac{\partial^2 f_i}{\partial v_\parallel^2}, \tag{30}$$

where we have linearized about the small number of particles in the escape region and assumed that terms containing $\partial f_i/\partial v_\parallel$ are larger than $\partial f_i/\partial v_\perp$.

[11] L. D. Landau, J. Phys. USSR 10, 25 (1946).

Here $\tau_{ei} = mv_{thi}/4\pi e^4 n_0 \lambda$, where λ is the Coulomb logarithm and v_{thi} is the thermal velocity of the Maxwellian distribution outside the escape region. We see immediately that the effective collision time, τ_{resi}, for particles near the hole is

$$\tau_{resi} = \tau_{ei}(\delta v_i/v_{thi})^2 \sim \tau_{ei}(2a/R). \tag{31}$$

The influence of collisions is very important if this time is smaller than the time, τ_i, required for resonant particles near the wall to leave the system,

$$\tau_{resi} \sim \frac{2a\tau_{ei}}{R} \lesssim \frac{\delta r}{v_{ei}} = \frac{R}{v_{thi}\theta}\left(\frac{2a}{R}\right)^{\frac{1}{2}} \tag{32a}$$

or

$$\theta\left(\frac{2a}{R}\right)^{\frac{1}{2}}\frac{\tau_{ei}v_{thi}}{R} < 1. \tag{32b}$$

We see that Coulomb collisions are more important than one would ordinarily think, and can cause particles to diffuse into the escape region. However, if collisions are still too infrequent, particles can still diffuse into the escape region since they scatter from turbulent electric fields which arise because the distribution function shown in Fig. 7 is unstable.

Let us then consider the stability of the electron distribution shown in Fig. 7. This distribution can be described approximately by the function

$$f_e(v_\parallel, v_\perp) = [1 - \Delta\psi_e(v_\parallel - V_\parallel^{(0)})]F_e(v_\parallel^2 + v_\perp^2), \tag{33}$$

where $\psi(v_\parallel - V_\parallel^{(0)})$ is a positive function and differs from zero only in the neighborhood of $V_\parallel^{(0)} = v_E/\theta$, so that

$$\psi(0) = 1, \qquad \int_{-\infty}^{\infty} dv_\parallel\ \psi(v_\parallel - V_\parallel^{(0)}) = \delta v_e. \tag{34}$$

The parameter Δ changes from unity to zero as the escape region is filled. The distribution of the main body of particles is chosen as Maxwellian

$$F_e(v_\parallel^2 + v_\perp^2) = \frac{n_0(r)}{(2\pi v_{the}^2)^{\frac{3}{2}}} \cdot \exp\left(\frac{-[v_\parallel^2 + v_\perp^2 - (2e/m_e)\Phi(r)]}{2v_{the}^2}\right), \tag{35}$$

where in the normalization constant we neglect the contribution from the escape region. First we check the stability of the electron distribution with respect to the longitudinal electron oscillations propagating along the magnetic field when the phase velocity is in the region

$$v_{the} \gg (\omega/k) \doteq V_\parallel^{(0)}, \qquad \gamma \gg k\ \delta v_e. \tag{36}$$

The dispersion relation for this oscillation is

$$1 - \frac{\omega_{pe}^2}{k^2}\int_{-\infty}^{\infty}\frac{dv_\parallel\ (\partial f_e/\partial v_\parallel)}{v_\parallel - \omega/k} = 0. \tag{37}$$

Expanding the integral in the range given by Eq. (36), we rewrite Eq. (37) as

$$1 + \frac{\omega_{pe}^2}{k^2 v_{the}^2} + \frac{\omega_{pe}^2\ \Delta F(V_\parallel^{(0)})}{[\omega - kV_\parallel^{(0)}]^2} \cdot\int_{-\infty}^{\infty}\psi_e(v_\parallel - V_\parallel^{(0)})\ dv_\parallel = 0. \tag{38}$$

This equation has an unstable solution with the growth rate

$$\gamma = \frac{\omega_{pe}}{(1 + \omega_{pe}^2/k^2 v_{the}^2)^{\frac{1}{2}}} \cdot\left(\Delta F(V_\parallel^{(0)})\int_{-\infty}^{\infty} dv_\parallel\ \psi_e(v_\parallel - V_\parallel^{(0)})\right)^{\frac{1}{3}} > k\ \delta v_e. \tag{39}$$

For small k, $\gamma = k(\Delta\delta v_e v_{the})^{\frac{1}{2}}$ and for large k,

$$\gamma = \omega_{pe}(\Delta\ \delta v_e/v_{the})^{\frac{1}{2}},$$

which is the maximum growth rate of this instability.

The ion distribution is unstable with respect to the ion cyclotron oscillations. The dispersion equation for electrostatic oscillations in an anisotropic plasma was derived by Harris[12] and has a form

$$1 + \sum_i \frac{\omega_{pi}^2}{k^2} \cdot\left\{\int_{-\infty}^{\infty} f_i(v_\perp = 0)\ dv_\parallel + \sum_{l=-\infty}^{\infty}\int_{-\infty}^{\infty} dv_\parallel \int_0^{\infty} dv_\perp\ v_\perp J_l^2\left(\frac{k_\perp v_\perp}{\omega_{ci}}\right) \cdot\frac{\{\omega v_\perp^{-1}(\partial/\partial v_\perp) + k_\parallel v_\parallel[v_\parallel^{-1}(\partial/\partial v_\parallel) - v_\perp^{-1}(\partial/\partial v_\perp)]\}f_i(v_\perp, v_\parallel)}{\omega - l\omega_{ci} - k_\parallel v_\parallel + i\epsilon}\right\} = 0. \tag{40}$$

Again for a phase velocity within the interval

$$(\omega - l\omega_{ci})/k_\parallel \simeq V_\parallel^{(0)}, \qquad \gamma \gg k_\parallel\ \delta v_\parallel,$$

we find by expanding the integrals in Eq. (40),

$$1 + \frac{\omega_{pi}^2}{k^2 v_{thi}^2}\left[\left(1 + \frac{T_i}{T_e}\right) - \int_{-\infty}^{\infty}\frac{\omega F(v_\parallel)\ dv_\parallel}{\omega - l\omega_{ci} - k_\parallel v_\parallel}\Gamma_l + \frac{k_\parallel^2 v_{thi}^2\ \Delta F(V_\parallel^{(0)})}{(\omega - l\omega_{ci} - k_\parallel V_\parallel^{(0)})^2}\int_{-\infty}^{\infty} dv_\parallel\ \psi_i(v_\parallel - V_\parallel^{(0)})\Gamma_l\right] = 0, \tag{41}$$

$$\Gamma_l = I_l(k_\perp^2 r_{Li}^2)\exp(-k_\perp^2 r_{Li}^2).$$

[12] E. G. Harris, J. Nucl. Energy C2, 138 (1961).

This equation first discussed by Galeev[13] has the same kind of solution as Eq. (38) in the limit

$$k_\perp r_{Li} \lesssim 1.$$

The expression for the growth rate is very similar to the one derived for the electron oscillation,

$$\gamma = \frac{k_\parallel v_{thi}[\Delta F(V_\parallel^{(0)})\Gamma_i(k_\perp^2 r_{Li}^2)\int_{-\infty}^{\infty}\psi_i(v_\parallel - V_\parallel^{(0)})\,dv_\parallel]^{\frac{1}{2}}}{(1 + T_i/T_e + k^2\lambda_{Di}^2)^{\frac{1}{2}}} > k_\parallel\,\delta v_i, \qquad (42)$$

where $\lambda_{Di} = v_{thi}/\omega_{pi}$ is the ion Debye length.

Let us note that the distribution function considered in Sec. IVA is stable with respect to a Harris type instability because for this case

$$\int \psi_i(v_\parallel - V_\parallel^{(0)})F_i(v_\parallel)\,dv_\parallel = 0,$$

and a velocity space gradient is now not a strong enough instability mechanism.

V. QUASI-LINEAR BEHAVIOR OF PLASMA SURFACE

Let us now qualitatively consider how the plasma surface adjusts to the wall. Initially we assume that the plasma touches the wall and therefore the plasma density near the wall is comparable with the plasma density at the center of the trap. Then, under the condition that the diffusion in velocity space is rapid enough to fill the velocity space hole during the escape time $\tau_j \equiv \delta r_j/v_{oj}$, the particle flux can be estimated as

$$J_j = (2\pi)^2 Rav_{oj}n_0(a, t)\int_{-\infty}^{\infty} dv_\parallel\,\psi(v_\parallel - V_\parallel^{(0)})F(v_\parallel). \qquad (43)$$

Because of the rapid filling of the escape region due to instability, the density of the resonant particles $n_0^{res}(a, t)$ is assumed the same as the nonresonant particles $n_0(a, t)$. Furthermore, the loss of particles of the jth specie takes place only in a small layer of width δr_j, near the wall. From Eq. (43) it follows that the rate of particle loss from the plasma column has a strong dependence on the number of resonant particles and hence on the electric field. On the other hand, due to the difference in the loss rate of electrons and ions, there arises a charge density which determines the electric field through the Poisson equation

$$\frac{1}{r}\frac{d}{dr}r\frac{d}{dr}\phi_0(r, t) = 4\pi e[n_i(r, t) - n_e(r, t)]. \qquad (44)$$

In order to find the electric field one must solve the self-consistent system of Eq. (44) and the equation for particle loss. This problem has been solved numerically by Bishop and Smith[6] for the case where particles move only along their adiabatic trajectories and some of these trajectories intersect the wall. For the turbulent case even to write the exact form of Eq. (43) for the particle flux is difficult, and we restrict ourselves to order of magnitude estimates. If the Debye length λ_D is smaller than ion trajectory dimensions $\lambda_D \ll \delta r_i$, the plasma in the layer of width δr_i is quasi-neutral. Hence the flux due to ions and electrons must be equal at the wall. Since very near the wall the flux due to nonresonant ions would dominate without an electric field, an electric field must arise to ensure the equality of the electron and ion fluxes. This electric field moves the resonant ion region toward the ion distribution tail while hardly affecting the electron resonance region, since $v_{thi} \lesssim v_E/\theta \ll v_{the}$.

Now the electron flux arises only from particles a distance δr_e from the wall. Hence eventually a large electron density gradient arises near the wall. As we have shown in Sec. III, this density profile becomes unstable under the condition given in Eq. (28), which for the present case has the form

$$\alpha(t) = \frac{r_{Le}}{\theta}\frac{n(a - \delta r_e, t) - n(a, t)}{\delta r_e n(a, t)}\left(\frac{r}{R}\right)^{\frac{1}{2}} > \left(\frac{r}{R}\right)^{\frac{1}{2}}. \qquad (45)$$

As soon as the electric field fluctuation appears in a plasma due to the instability, the longitudinal invariant for electrons is no longer conserved. Therefore, the electron orbits diffuse in coordinate space. Again, as an estimate, we set the effective collision frequency for the resonant electrons equal to the growth rate of the instability given by Eq. (28),

$$\nu_{eff} = \gamma_k \sim \omega_{pe}\left(\alpha(t)\frac{\delta v_e^2}{v_{the}^2}\right)^{\frac{1}{3}}. \qquad (46)$$

Then in order to balance the particle diffusion with direct loss of particles from the escape region, the density gradient must almost equal the marginally stable one. Using this condition we obtain the density gradient near the wall at the moment when the density of the electrons is zero at the wall (see Fig. 8)

$$r_{Le}/\theta\,\Delta r_e \approx 1, \qquad (47)$$

where we put $n(a - \Delta r_e) \approx n(a)$, because for our case $a \gg \Delta r_e$.

The time of the relaxation, t_e, to this state can be estimated if we divide the number of particles leaving the trap by the particle flux to the wall

$$t_e = \frac{(2\pi)^2 Ra\,\Delta r_e n(a)}{J_e} = \frac{R^{\frac{3}{2}}}{v_{the}\theta r^{\frac{1}{2}}}. \qquad (48)$$

[13] A. A. Galeev, Institute of Nuclear Physics, Novosibirsk Preprint 10 (1966).

During this time the electron loss and the electric field are described, respectively, by Eqs. (43) and (44).

After this time, the electron distribution becomes stable, but the resonant ions within a distance δr_i from the edge continue to leave the trap because their trajectories intersect the wall and thus the electric field continues to increase. The value of the electric field at the final state $t \to \infty$ can be found from the stability conditions for an ion distribution with an empty escape region

$$\exp(-v_E^2/2\theta^2 v_{thi}^2) = (r/R)^{\frac{1}{2}}. \qquad (49)$$

In our picture it is implicitly assumed that

$$r/R < (T_e m_e/T_i m_i)^{\frac{1}{2}}.$$

For this case there are more electrons in the layer Δr_e than resonant ions in δr_i, and the electric field is determined by Eq. (49). Charge neutrality is established since the turbulence causes ions to be replenished from the surrounding reservoir. However, for the reversed inequality more ions are lost, and consequently, to maintain charge neutrality the electric field must be larger than that given by Eq. (49). The final electric field is then determined by the charge neutrality condition, $\Delta r_e n(a) = \delta r_i n(a)\int dv_\parallel \psi F$, which yields

$$\exp\left[-\frac{v_E^2}{2\theta^2 V_{thi}^2}\right] \sim \left(\frac{T_e m_e}{T_i m_i}\right)^{\frac{1}{2}}\frac{R}{r}. \qquad (50)$$

Thus we conclude that for the case under consideration here, $r_{Li} < \delta r_i < a$, the fractional loss of particles due to the wall is small as $\Delta r_e/a$ and the electric field, defined by the larger value implied by Eq. (49) or (50), appears only in the narrow layer of width δr_i near the wall (see Fig. 8). The voltage, V, across this layer can be estimated using $V_E \sim v_{thi}$, and we find $V \sim e^{-1}(a/R)^{\frac{1}{2}}T_i$.

Finally, we note that in the case of a relatively weak rotational transform the instability given by Eq. (28), which is driven by ions, is present throughout the plasma. This instability should cause an enhanced diffusion, and hence loss of ions, so that an electric field forms throughout the plasma. The electric field shifts the resonant region to the tail of the distribution function and stability should occur when

$$(r_{Li}R/ar_L)\exp(-v_E^2/2v_{thi}^2\theta^2) < 1. \qquad (51)$$

Let us now note that the electric field given by Eqs. (49)–(51) stabilizes only the fast velocity space instabilities considered in Sec. IV. Still other instabilities due to the anomalous nature of the distribution function are possible, and they may not be stabilized by the electric field. For example, the growth rate of the universal instability can be altered since the instability can be driven by the trapped electrons whose resonant velocity is small even with an electric field present.

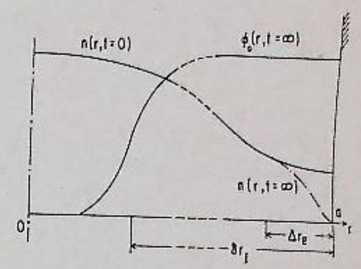

FIG. 8. Particle density and electric field profile.

The dispersion relation for the low frequency drift modes ($\omega \ll \omega_{ci}$) with wavelengths larger than the ion Larmor radius has the form[14]

$$1 + \frac{T_i}{T_e} - \frac{\omega - \mathbf{k}\cdot\mathbf{v}_g^i - k_\phi v_d^i}{\omega - \mathbf{k}\cdot\mathbf{v}_g^i}(1 - k_\perp^2 r_{Li}^2)\frac{-i\pi T_i}{m_e\,|k_\parallel|\,n_0} \cdot\left(k_\parallel\frac{\partial f_e(x, v_\parallel)}{\partial v_\parallel} + \frac{k_\phi}{\omega_{ce}}\frac{\partial f_e}{\partial r}\right)_{v=\omega-\mathbf{k}\cdot\mathbf{v}_g/k_\parallel} = 0, \qquad (52)$$

where

$$v_d^i = \frac{v_{thi}^2}{\omega_{cn}}\frac{dn}{dr}, \qquad \mathbf{v}_g^i = \frac{v_{thi}^2\hat{\mathbf{x}}}{R\omega_{ci}},$$

k_ϕ is the azimuthal component of the wave vector and $|k_\parallel|\,v_{the} > \omega > |k_\parallel|\,v_{thi}$. It follows from Eq. (52) that for a Maxwellian, plasma instability only arises because of the finite Larmor radius correction, and therefore the growth rate decreases rapidly for the long waves $k_\perp^2 r_{Li}^2 \ll 1$. In a curved magnetic field even without finite Larmor radius effects, there appear two additional destabilizing effects. One is due to the frequency shift because of the curvature drift,[15] and the other comes from the change of the slope of the velocity distribution. The expression for the growth rate then is given by

$$\gamma_k = (\tfrac{1}{2}\pi)^{\frac{1}{2}}\frac{\omega^2}{|k_\parallel|\,v_{the}}\left\{\left[k_\perp^2 r_{Li}^2 - \frac{(\mathbf{k}\cdot\mathbf{v}_g^i)(\hat{\mathbf{x}}\cdot\mathbf{b})}{k_\phi V_d^i}\right]\left(1 + \frac{T_e}{T_i}\right) - \frac{k_\parallel v_{the}}{\omega}\frac{r_{Le}}{\theta}\frac{d\ln n}{dr}\left(\frac{r}{R}\right)^{\frac{1}{2}}\right\}. \qquad (53)$$

In our calculations we have used straight particle trajectories, which means that instability's develop-

[14] A. A. Galeev, S. S. Moiseev, and R. Z. Sagdeev, At. Energ. 15, 451 (1963) [English transl.: J. Nucl. Energy C6, 645 (1964)].

[15] A. A. Galeev, Zh. Eksperim. i Teor. Fiz. 44, 1920 (1963) [English transl.: Soviet Phys.—JETP 17, 1292 (1963)].

ment is sufficiently rapid if $\gamma\delta\tau_i > 1$. This condition breaks down in the case of large shear

$$(r_{Li}/r\theta)^2 > (m_i r/m_e R)^{\frac{1}{2}}.$$

If the curvature influence on the growth rate is larger than the finite Larmor radius effect, the drift waves are purely growing in a coordinate system moving with velocity $(v_d^e + v_o^i)$. If we estimate the coefficient of ambi-polar diffusion as in the case of strong turbulence,[16] then $D_\perp \sim \gamma_k k_r^{-2}$. The main contribution to the diffusion comes from long waves, $k_\phi^{-1} \sim k_r^{-1} \sim L$. If the last term in Eq. (53) is largest, then the trapped particles determine the instability, and we find

$$D_\perp \sim \frac{r_{Le}}{\theta}\left(\frac{r}{R}\right)^{\frac{1}{2}} \frac{d(\ln n)}{dr}\frac{v_{the}^2}{\omega_{ce}}. \tag{54}$$

Thus even in the presence of an electric field the plasma slowly diffuses to the wall due to the drift instability.

Still other instabilities can probably be found, besides the ones we have discussed. In general, an electric field will develop if the instability interacts primarily with only one specie so that ambi-polar diffusion does not occur. If in our model the fast instabilities can be stabilized in a time scale short compared with instabilities driven by two species (like the drift mode), an electric field always arises. Ambi-polar diffusion then takes place on the time scale of the slower instabilities.

[16] B. B. Kadomtsev, Zh. Eksperim. i Teor. Fiz. 43, 1688 (1962) [English transl.: Soviet Phys.—JETP 16, 1191 (1963)].

VI. SUMMARY

We have discussed some velocity space instabilities present in a toroidal machine and have given a nonlinear picture of how the instabilities saturate. Our results are very optimistic for toroidal confinement, since the instabilities saturate rapidly and the remaining relaxation is on a long time scale, the curvature drift time. Further, there exists a final state in which the majority of the particles are still trapped and the system is stable.

In our analysis we have neglected many other instabilities like interchange, drift and resistive modes that contribute to the instability of present devices but can hopefully be eliminated in the future. Present machines give rise to Bohm diffusion which produces a particle flux rate that is much faster than that produced by the curvature drift, and hence our quasi-linear picture probably fails for these devices.

ACKNOWLEDGMENTS

It is a pleasure to thank M. N. Rosenbluth and R. Z. Sagdeev, for originally suggesting the investigation of this problem and for many subsequent discussions; J. B. Taylor, for a discussion about particle orbits; and Abdus Salam and the International Atomic Energy Agency, for their hospitality during our pleasurable sojourn at the International Centre for Theoretical Physics, Trieste.

This work supported in part by the United States Atomic Energy Commission.

Effect of Pressure on Negative V'' Stellarators

JOHN L. JOHNSON*
Plasma Physics Laboratory, Princeton University, Princeton, New Jersey
(Received 2 June 1966)

Stability with respect to hydromagnetic interchanges can be achieved in closed configurations if $V''(\psi) < 0$ with $V''(\psi)$ the volume inside a magnetic surface of flux ψ. A low-pressure expansion is used to examine the effects of plasma currents in a negative V'' configuration which utilizes an $l = 2$ shaping field and an $l = 1$, $l = 3$ corrugating field and in which toroidal curvature is neglected. Numerical calculations indicate that the effect on stability of these currents is small. Since the basic features of all the proposed negative V'' configurations are similar, this strengthens the belief that vacuum field considerations provide an adequate approximation.

IN closed hydromagnetic systems, interchange instability modes are stabilized if $V''(\psi) < 0$ when the pressure is sufficiently small.[1] As the pressure is increased $V''(\psi)$ is changed in two ways: The material pressure displaces some magnetic field outward and thus, by providing a diamagnetic current, decreases $V''(\psi)$. Currents must flow along the magnetic field lines to prevent charges from building up due to drifts associated with the curvature of the magnetic field lines. The fields associated with these currents can change $V''(\psi)$ by distorting the shapes of the magnetic surfaces.

Stability analyses[2] indicate that the part of $V''(\psi)$ associated with the diamagnetic current does not enter the stability criterion. Material pressure affects the stability problem then through the currents along the magnetic field lines and can be studied by analyzing the variation with pressure of $V''(\psi) - V_\beta''(\psi)$, where $V_\beta''(\psi)$ is due to the diamagnetic current. This is done here for a particular negative V'' stellarator configuration.[3,4] The work closely follows that of Greene and Johnson.[5]

The magnetic field is given by

$$\mathbf{B} = B^{(0)}\nabla\Big\{z + \frac{\epsilon_2}{2\gamma} I_2(2\gamma r)\sin 2u + \sum_{l=1,3}\frac{\epsilon_l}{h + l\gamma} I_l[(h + l\gamma)r]\sin(lu - hz)\Big\} + \mathbf{e}_z B^{(\beta)}(\Psi^{(0)}) + B^{(0)}\nabla\times\mathbf{e}_z A^{(\sigma)}(r,u) + \cdots, \tag{1}$$

$$u \equiv \theta - \gamma z, \quad \epsilon_1^2 \sim \epsilon_1\epsilon_3 \sim \epsilon_3^2 \sim \gamma/h \sim B^{(\beta)}/B^{(0)} \sim hA^{(\sigma)} \ll 1, \quad hr \sim \epsilon_2 \sim 1.$$

The first three terms are the uniform field, the shaping field, and the corrugator field of Johnson *et al.*,[3,4] $B^{(\beta)} = p^{(\beta)}(\Psi^{(0)})/B^{(0)}$ is associated with diamagnetic currents, and $A^{(\sigma)}$ is due to current along the magnetic field lines. In lowest order

$$\sigma \equiv \mathbf{J}\cdot\mathbf{B}/B^2 = (-1/4\pi B^{(0)})\nabla^2 A^{(\sigma)}. \tag{2}$$

Equation (2), together with the boundary condition that there be no current outside the plasma associated with $A^{(\sigma)}$, can be written in the form of an integral equation,[5]

$$A^{(\sigma)}(r,u) = B^{(0)}\int_0^{2\pi}\int_0^\infty g(r,u;r',u')\cdot\sigma(r',u')r'\,dr'\,du', \tag{3}$$

$$g(r,u;r',u') = -2\ln\left(\frac{r}{r'}\right) + \sum_{n>0}\frac{2}{n}\left(\frac{r'}{r}\right)^n\cos n(u-u') \quad (r' \le r)$$
$$= \sum_{n>0}\frac{2}{n}\left(\frac{r}{r'}\right)^n\cos n(u-u') \quad (r' \ge r). \tag{4}$$

Straightforward order-by-order solution of the equation for a magnetic surface, $\mathbf{B}\cdot\nabla\Psi = 0$, leads to an expression for the zeroth-order surface[4]

$$\Psi^{(0)} = \frac{LB^{(0)}}{2}\left[\gamma r^2\left(1 - \frac{\epsilon_2}{2}\cos 2u\right) - \sum_{l,m}\frac{m\epsilon_l\epsilon_m}{h^2 r}\cdot I_l'(hr)I_m(hr)\cos(l-m)u + A^{(\sigma)}(r,u)\right]. \tag{5}$$

Similarly, the requirement that $\nabla\cdot\mathbf{J} = 0$ determines the current along the field lines;[5]

$$\sigma = \frac{Lp^{(\beta)\prime}(\Psi^{(0)})}{B^{(0)}}\left(\Omega - \frac{\oint \Omega\, ds/|\nabla\Psi^{(0)}|}{\oint ds/|\nabla\Psi^{(0)}|}\right), \tag{6}$$

$$\Omega \equiv \tfrac{1}{2}\sum_{l,m}\epsilon_l\epsilon_m\left[I_l'(hr)I_m'(hr) + \frac{lm + h^2r^2}{h^2r^2}I_l(hr)I_m(hr)\right]\cos(l-m)u, \tag{7}$$

* On loan from Westinghouse Research Laboratories.

[1] A. Lenard, Phys. Fluids 7, 1875 (1964).

[2] J. L. Johnson and J. M. Greene, J. Nucl. Energy (to be published); see also I. B. Bernstein, E. A. Frieman, M. D. Kruskal, and R. M. Kulsrud, Proc. Roy. Soc. (London) A244, 17 (1958), and J. L. Johnson, C. R. Oberman, R. M. Kulsrud, and E. A. Frieman, Phys. Fluids 1, 281 (1958).

[3] J. L. Johnson, Phys. Fluids 7, 2015 (1964).

[4] J. L. Johnson, U. R. Christensen, E. A. Frieman, and D. Mosher, J. Nucl. Energy C8, 361 (1966).

[5] J. M. Greene and J. L. Johnson, Phys. Fluids 4, 875 (1961).